PCCP

Accepted Manuscript

ROYAL SOCIETY OF CHEMISTRY

www.rsc.org/pccp

TOC:

Connecting Carbon Nanotubes to Polyoxometalate Clusters for Engineering High-Performance Anode Materials

Wei Chen, Lujiang Huang, Jun Hu, Feifei Jia, and Yu-Fei Song*

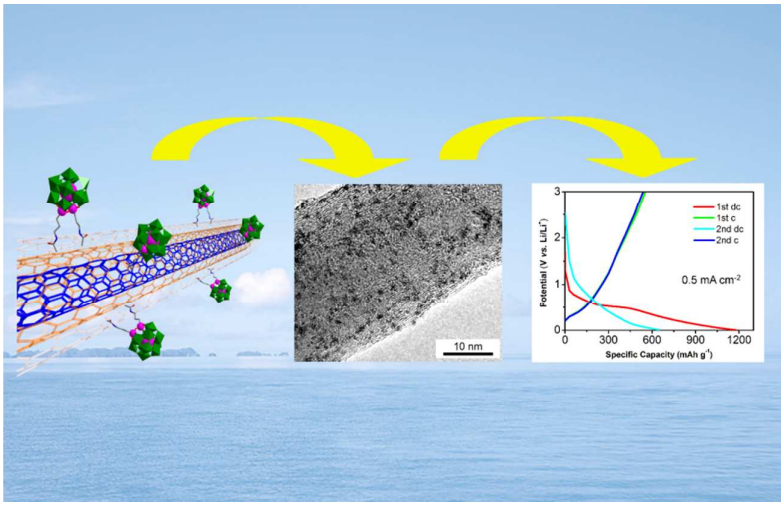

Cite this: DOI: 10.1039/c0xx00000x

www.rsc.org/xxxxxx

ARTICLE TYPE

Connecting Carbon Nanotubes to Polyoxometalate Clusters for Engineering High-Performance Anode Materials**

Wei Chen,† Lujiang Huang,† Jun Hu, Tengfei Li, Feifei Jia, and Yu-Fei Song*

Received (in XXX, XXX) Xth XXXXXXXXX 20XX, Accepted Xth XXXXXXXXX 20XX

DOI: 10.1039/b000000x

Abstract: Carbon nanotubes (CNTs) possess excellent structural and electronic properties, and have been widely investigated as anode materials. Polyoxometalates (POMs) exhibit superior physical properties such as electronic versatility, redox character and unique molecular structures. In this paper, covalent modification of carbon nanotubes (CNTs) with organosilica-containing polyoxometalate (POM) of $[Bu_4N]_4[SiW_{11}O_{39}\{O(SiCH_2CH_2CH_2NH_2{\bullet}HCl)_2\}]$ (SiW_{11}-NH_2) leads to the formation of the nanocomposite material of CNTs-SiW_{11}, which has been characterized by FT-IR, XRD, HR-TEM, XPS and Raman spectrum etc. At a current density of 0.5 mA cm^{-2}, the application of CNTs-SiW_{11} nanocomposite as anode material in lithium battery exhibits the 1st discharge capacity of 1189 mAh g^{-1}, and the 2nd discharge capacity of 650 mAh g^{-1}, which remains stable for up to 100 cycles. The CNTs-SiW_{11} nanocomposite exhibits high discharge capacity, good capacity retention and cycling stability.

Introduction

Carbon nanotubes (CNTs) have attracted wide attention with the the determination of the unique physical and chemical properties.[1-4] Recent efforts have been focusing on the development of CNTs-containing functional materials and the investigation of potential application. Among so many trials, chemical functionalization of CNTs[5,6] is particularly interesting since it can not only increase solubility of CNTs, but also develop advanced multifunctional materials.[7] Meanwhile, it is noted that the combination of different materials with CNTs has resulted in the formation of a number of new functionalized CNTs with unprecedented properties.[8] With their unique one-dimensional structure, high electrical and thermal conductivities, large surface area and outstanding mechanical properties, CNTs have been considered as ideal materials to improve the electrochemical properties of electrode materials for lithium ion batteries (LIBs) with enhanced energy conversion and storage capacities. Recent development of LIBs has involved design of CNTs-based nanocomposites for electrode materials to make better use of attractive properties of CNTs.

Polyoxometalates (POMs) represent an unmatched range of architectures and chemical properties. As transferable building blocks, POMs can be covalently modified in a predefined manner, which allows the development of sophisticated assemblies, multi-functional materials and devices.[9-12] Recently, the investigation of POMs-modified CNTs has become a fascinating subject. For example, Biochio *et al* reported efficient water oxidation can be performed at the POM/CNTs interfaces[13]. Giusti *et al* developed new POMs/SWNTs (single-walled nanotubes) magnetic materials.[14] Awaga *et al*. reported the first nanohybrid system of $[PMo_{12}O_{40}]^{3-}$/SWNTs[15] as cathode material with high battery capacity, and later on, they confirm the POMs can act as electron sponges using the in-operando X-ray absorption fine structure studies.[16] Recently, we reported the first example of covalently tethered polyoxometalate-pyrene hybrids for non-covalent sidewall functionalization of SWNTs as anode material.

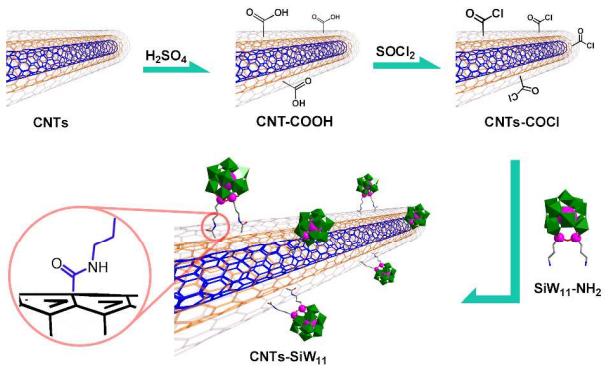

Sheme 1 Synthesis of Carboxyl-functionalized CNTs (CNTs-COOH), acyl chloride-functionalized CNTs (CNTs-COCl) and CNTs-SiW_{11}.

Given the excellent structural and electronic properties of CNTs and POMs, the development of POMs modified CNTs as electrode materials for LIBs have attracted wide attention.

Compared with non-covalent modification of CNTs, the covalent bonding results in the formation of stable link between POMs and CNTs, and can induce more sidewall defects[17] and thereby more pathways for Li^+ transfer. Nevertheless, almost all the POMs modified CNTs examples reported so far exhibit the non-covalent interactions between POMs and CNTs. As such, the scientific question is whether it is possible to connect the POMs onto CNTs *via* covalent bonds and how is the performance of the resultant nanocomposite as electrode materials. In this paper, we have reported for the first time by covalently grafting SiW_{11}-NH_2 ($[Bu_4N]_4[SiW_{11}O_{39}\{O(SiCH_2CH_2CH_2NH_2{\bullet}HCl)_2\}]$) onto CNTs, and the resulting CNTs-SiW_{11} nanocomposite shows excellent electrochemical performance with the high discharge capacity, good capacity retention and cycling stability.

Experimental Section

All the starting materials and reagents were purchased from Alfa Aesar Company and were used as supplied without further purification. The solvents used in the reactions were dried according to standard procedures. All reactions were carried out under N_2 atmosphere and anhydrous conditions.

$[Bu_4N]_4[SiW_{11}O_{39}\{O(SiCH_2CH_2CH_2NH_2{\bullet}HCl)_2\}]$ (denoted as SiW_{11}-NH_2) was synthesized and described previously.

Synthesis of carboxyl-functionalized carbon nanotubes (denoted as CNTs-COOH): This compound was prepared as described previously with slight modification. 100 mg of CNTs was added to the H_2SO_4/HNO_3 (3:1 by volume) solution with vigorous stirring. The flask was then immersed in an ultrasonic bath for 30 min, and the mixture was stirred for 3 h under reflux. After cooling to room temperature, the mixture was diluted with 100 mL of deionized water and then vacuum-filtered through a glass filter. The filtered solid was washed with deionized water until the pH of the filtrate close to 7. After that, the solid was washed with 50 mL of THF and acetone, respectively. And it was further dried under vacuum for 24 h at 120 °C, giving 72 mg of CNTs-COOH.

Synthesis of acyl chloride-modified carbon nanotubes (denoted as CNTs-COCl): The as-prepared CNTs-COOH (50 mg) reacted with excess amount of $SOCl_2$ (10 mL) for 24 h under reflux at 60-70 °C. After that, the reaction mixture was evaporated under vacuum to give the CNTs-COCl, which was immediately used for the next step reaction without further purification.

Preparation of CNTs-SiW_{11}: In a 100 mL round-bottomed flask under nitrogen, CNTs (20 mg) was dispersed in MeCN (60 mL) using an ultrasonic bath. Then Et_3N (0.5 mL) was added to the solution and it wa degassed under vacuum, purged with nitrogen for three times to remove the oxygen and then cooled to 0 °C. A solution of 1 g of SiW_{11}-NH_2 in MeCN (10 mL) was added to the flask for 30 min. The temperature was keep at 0 °C for 2 h, and then heated to 70 °C for 24 h. After that, the resulting mixture was cooled to room temperature, and it was filtered through a 200 □m filter and wash with MeCN to remove the excess amount of SiW_{11}-NH_2. The final product was dried under vacuum at 120 °C for 3 days.

Results and Discussion

To engineer the POMs modified CNTs as anode material, CNTs was oxidized by H_2SO_4/HNO_3 firstly and then treated with $SOCl_2$, to which the POM cluster of SiW_{11}-NH_2 was added.[18,19] The resulting SiW_{11}-NH_2 modified CNTs has been characterized by using different spectroscopic techniques. The obtained nanocomposite material has been washed thoroughly with pure CH_3CN to insure that the SiW_{11} won't be adsorbed on CNTs by electrostatic interaction because of the high solubility of SiW_{11} in polar solvents such as CH_3CN. By doing so, only covalently grafted SiW_{11} onto CNTs can be formed with the amide bonds. FT-IR spectra of SiW_{11}-NH_2, carboxyl-functionalized carbon nanotubes (CNTs-COOH) and CNTs-SiW_{11} provide evidence for the characteristic vibrations of the attached groups. As shown in Figure 1a, FT-IR spectrum of CNTs-COOH shows a very broad stretching band for hydroxyl groups at 3450 cm^{-1}, and the ν(C=O) stretching of carboxyl groups at 1628 cm^{-1}. The characteristic ν(W=O) and ν(W-O-W) stretching bands can be observed at 748 cm^{-1}, 808 cm^{-1} in SiW_{11}-NH_2. In contrast, FT-IR spectrum of CNTs-SiW_{11} exhibits the ν(N-H) and ν(C-H) can be seen at 3321 cm^{-1} and 2970-2848 cm^{-1}, respectively; A strong characteristic ν(C=O) stretching band at 1631 cm^{-1}, ν(N-H) at 1550 cm^{-1} and the ν(C-N) at 1296 and 1213 cm^{-1} correspond to amide bond, which indicates the formation of amide bonds between CNTs and POMs, and the ν(W=O) and ν(W-O-W) stretching bands can also been found at 770 cm^{-1}, 824 cm^{-1}, which means the structure of SiW_{11} maintained during covalently connected to CNTs.

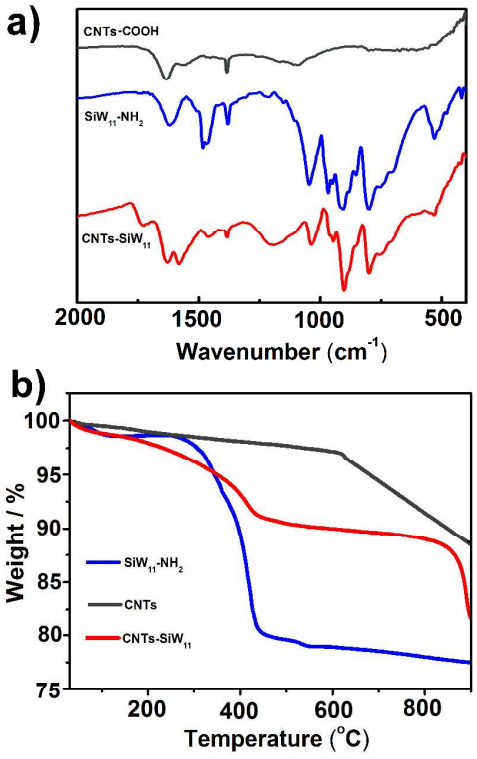

Fig. 1 a) FT-IR spectra of CNTs-COOH, SiW_{11}-NH_2 and CNTs-SiW_{11}. b) TGA measurements of CNTs, SiW_{11}-NH_2 and CNTs-SiW_{11}.

Thermal-gravimetric analysis (TGA) of SiW_{11}-NH_2, CNTs and CNTs-SiW_{11} has been presented in Figure 1b. It can be seen that the pristine CNTs do not exhibit any decomposition before 600 °C, while the SiW_{11}-NH_2 and CNTs-SiW_{11} nanocomposites show the weight loss of 28.26 and 7.24 wt%, respectively. If a similar weight loss behavior of SiW_{11}-NH_2 and CNTs is assumed to take place, the SiW_{11}-NH_2 content in the CNTs-SiW_{11} nanocomposite can be roughly determined to be 45.13 wt%.[20]

Further characterization of the CNTs-SiW_{11} nanocomposite has been studied by X-ray photoemission spectroscopy (XPS). As shown in Figure 2a. The W(4f) photoemission peak can be clearly observed and shows two peaks from the spin orbital splitting of the $4f_{7/2}$ and $4f_{5/2}$ at 36.52 eV and 38.61 eV, respectively, which means no valence change of W in SiW_{11} during connected to the CNTs. The XPS analysis of C_{1s} spectra (Figure 2b) show detailed surface functional groups on the CNTs. An asymmetric peak from sp^2 hybridized carbons centred at 284.5 eV with an extended tail at the higher energy region is generated for CNTs-SiW_{11}. Using this asymmetric peak as a reference, the C_{1s} peak of the oxidized CNTs can be fitted to five Gaussian-Lorentzian shape peaks, which are attributed to sp^2 and sp^3 hybridized diamond-like carbons (284.55 and 284.98 eV), carbonyls C-O (286.46 eV), and carboxyls (O=C-OH), N-C=O (288.04 eV). The XPS analysis N_{1s} of CNTs-SiW_{11} (Figures 2d) clearly shows the presence of amide bonds N-C=O (288.04 eV in C_{1s} and 400.8 eV in N_{1s}), and residual amines NH_2 (NH_3^+) (286.2 eV in C_{1s} and 402.6 in N_{1s}), which indicates successful formation of amide bonds[21]

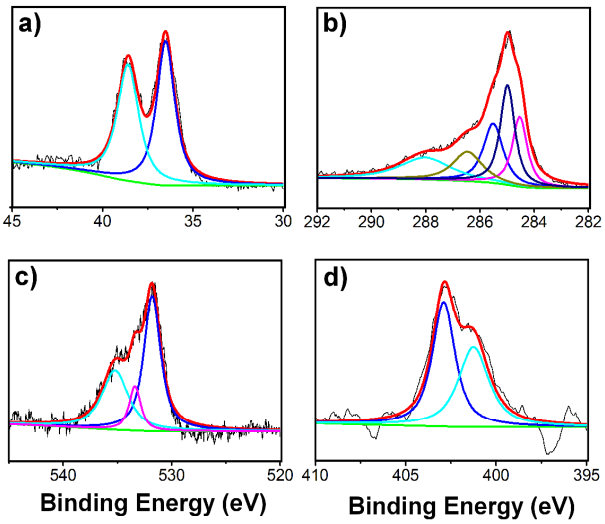

Fig. 2 XPS core level spectra of (a) W_{4f} bands; (b) C_{1s} bands; (c) O_{1s} bands; (d) N_{1s} bands.

As shown in Figure 3, Raman spectra show the tangential vibration mode (G band) and the acromial peaks[20b] at 1570, 1607 cm^{-1} for CNTs, 1573, 1602 cm^{-1} for CNTs-COOH and 1579, 1610 cm^{-1} for CNTs-SiW_{11}, respectively. Meanwhile, the disorder-induced D band shifts slightly from 1319 cm^{-1} in CNTs to 1324 cm^{-1} in CNTs-COOH and 1331 cm^{-1} in CNTs-SiW_{11}. Moreover, it is noted that for CNTs-COOH and CNTs-SiW_{11}, the intensity of D band is higher than that of G band, whereas the intensity of D band is much lower than that of G band in pristine CNTs. Such result in the CNTs-COOH and CNTs-SiW_{11} nanocomposite could be attributed to the surface defects of CNTs by oxidation under the H_2SO_4/HNO_3 solution to form carboxyl group. The relative intensity of D/G in CNTs-COOH and CNTs-SiW_{11} is alike, suggesting that the modification by SiW_{11}-NH_2 does not further damage the surface of CNTs. The second disordered D* band and the second vibration mode G* band shift significantly to higher frequency from 2639, 2894 cm^{-1} in CNTs, 2644, 2904 cm^{-1} in CNTs-COOH and to 2666, 2923 cm^{-1} in CNTs–SiW_{11} nanocomposite.

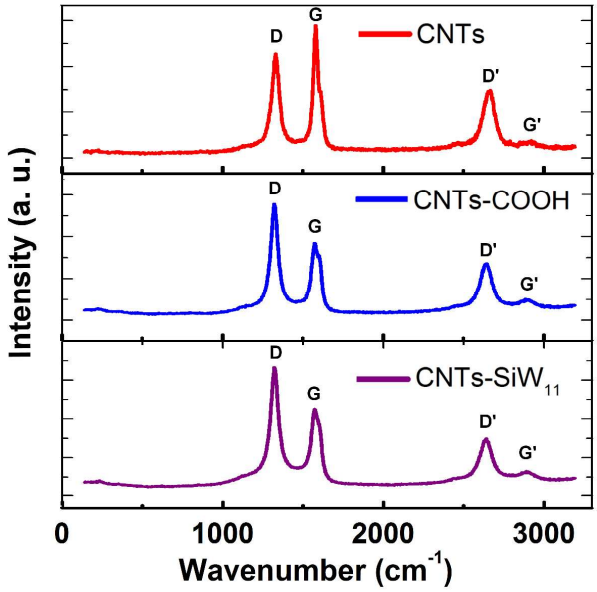

Fig. 3 Raman spectra of CNTs, CNTs-COOH and CNTs-SiW_{11}.

Figure 4 exhibits the morphological study of the CNTs and CNTs-SiW_{11} nanocomposite samples. SEM images show that the CNTs tend to aggregate together (Figure 4a), while the CNTs-SiW_{11} are found to be loosened (Figure 4b), indicating the improved dispersion of the latter samples. Figure 4c displays the stability of the CNTs and CNTs-SiW_{11} in organic solution. The CNTs solution forms a colorless clear solution, whereas the CNTs-SiW_{11} solution is still deep gray. TEM images of the pristine CNTs do not reveal any externally grafted objects (Figure 4d). In contrast, TEM images of the CNTs-SiW_{11} nanocomposite show the presence of bundles decorated by dark spots that can be clearly distinguished as SiW_{11} (Figure 4e). HR-TEM images (Figure 4f) clearly indicate that the CNTs have been modified by SiW_{11}. The small black point with a homogeneous dispersion around 1~2 nm can be define as a single SiW_{11} molecule. In addition, no free SiW_{11} molecules can be observed beyond CNTs, which suggest the successful immobilization of SiW_{11} onto CNTs. Energy dispersive X-ray (EDX) spectroscopy provides further evidences to confirm the presence of W on the surface of the CNTs, which is consistent with the XPS results.

Electrochemical properties of the CNTs-SiW_{11} nanocomposite

as anode material for lithium-ion batteries have been investigated. Figure 5a shows the charge-discharge voltage profiles of the CNTs-SiW_{11} nanocomposite electrode with the current density of 0.2 mA cm^{-2} for the first two cycles. The first discharge capacity of the CNTs-SiW_{11} electrode is 1527 mAh g^{-1}, and in the second cycle, the discharge capacity of 759 mAh g^{-1} is achieved. It should be noted that the capacities decrease in the first two cycles is due to the irreversible surface reactions on both electrodes.

Figure 5b shows the cycling stability and capacity retention of the CNTs-SiW_{11} electrode at the current density of 0.5 mA cm^{-2}. In the CNTs-SiW_{11} nanocomposite, the first discharge capacity is 1189 mAh g^{-1}, and then it exhibits the capacity decay from the second cycle.

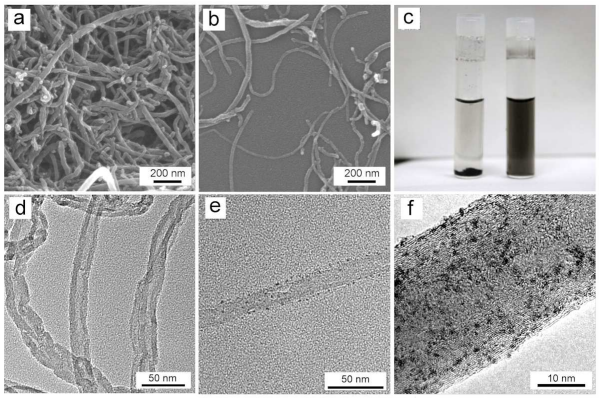

Fig. 4 SEM images of (a) CNTs and (b) CNTs-SiW_{11}; (c) The CNTs (left) and CNTs-SiW_{11} (right) in MeCN for one month; TEM images of (d) CNTs and (e) CNTs-SiW_{11}; (f) HR-TEM image of CNTs-SiW_{11}, and the black points is SiW_{11}.

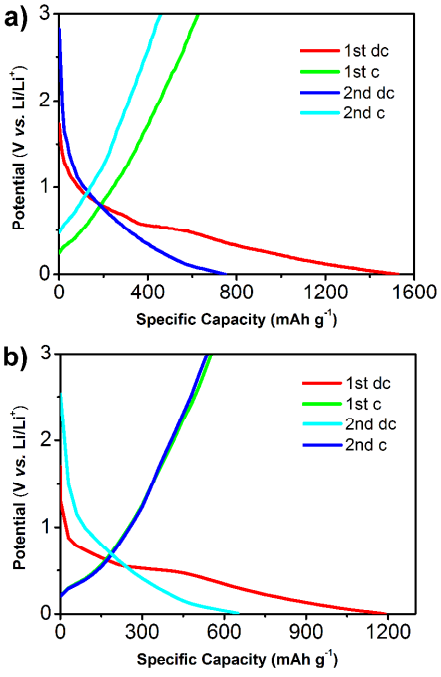

Fig. 5 a) The 1st and 2nd charging and discharging curves of the lithium battery; a) current density is 0.2 mA cm^{-2}.;b) current density is 0.5 mA cm^{-2}.

After 20 cycles, the capacity remains stable and a capacity of 650 mAh g^{-1} could be achieved after 100 cycles, with high capacity retention of 54.6%. Such a prominent difference between CNTs-SiW_{11} and the physical mixture of CNTs an SiW_{11}-NH_2 highlights the efficiency of the CNTs-SiW_{11} nanocomposite material as high-performance anode material. High electrode reversibility is another very important parameter for practical battery applications. And those of the following cycles are up to 99%. This result indicates that covalent functionalization of CNTs by SiW_{11} leads to the large enhancement of the performance as anode material when compared with the discharge capacity of 400~450 mAh g^{-1} by CNTs alone,[12] and that of 300 mAh g^{-1} by the physical mixture of CNTs and SiW_{11} with low capacity retention of 33.3%, indicating the important role of covalent connection of CNTs to SiW_{11} as showing in Figure 6.

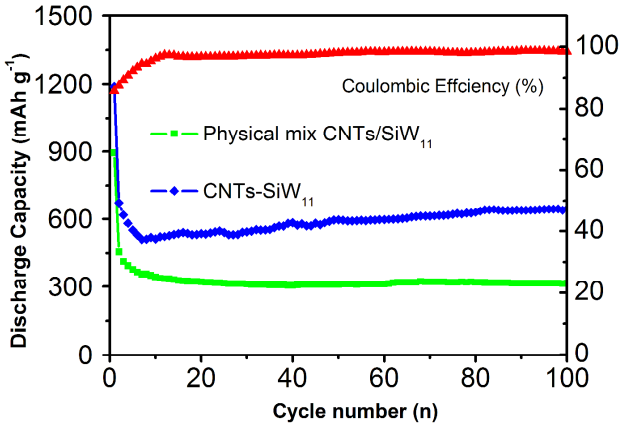

Fig. 6 Discharge capacity and coulombic efficiency vs cycle number of Physical mix CNTs/SW_{11} and CNTs-SiW_{11}; current density is 0.5 mA cm^{-2}.

The rate performance and the cycling stability during the lithium ion insertion/extraction processes are key factors for practical application. Herein, the rate capability of CNTs-SiW_{11} has been evaluated at various currents in the range of 0.05~1 mA cm^{-2} at the cut-off voltage between 0 and 3.0 V vs. Li^+/Li, and the results are presented in Figure 7a. The discharge capacities of 802, 770, and 704 mA h g^{-1} have been obtained at the current densities of 0.05, 0.1, and 0.2 mA cm^{-2}, respectively. The capacities at a higher current of 1 mA cm^{-1}, although, fading rapidly, could still deliver 584 mAh g^{-1}. Moreover, even after 70 cycles, when the current is restored to 0.05 mA cm^{-2}, the CNTs-SiW_{11} nanocomposite delivers 890 mAh g^{-1} without fading. The stable cycle performance of the CNTs-SiW_{11} nanocomposite at high rates indicates the ultra-fast solid-state diffusion of Li ions in bulk owing to the short diffusion path length and stable structure. Figure 7b shows the cyclic voltammograms of the CNTs-SiW_{11} nanocomposite at a scan rate of 0.1 mV s^{-1} over the range of 0-3 V. In the first cycle, an irreversible reduction peak at about 0.7 V

indicates the formation of solid electrolyte interphase (SEI), however, this peak disappears in the following cycles. The peak of 0.01-0.2 V in the reduction process is caused by the insertion of Li. The oxidation peak at 0.2 V shown in the charge process can be ascribed to the Li-extraction from the CNTs. Such Li-extraction process could be observed in the following cycles, suggesting the good reversibility of the CNTs-SiW_{11} nanocomposite.

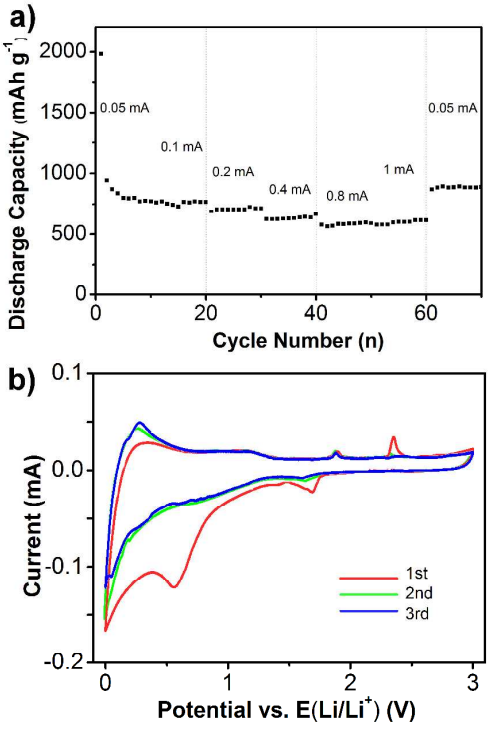

Fig. 7 a) Rate performance of the CNTs-SiW_{11} composite electrode at various current densities of 0.05, 0.1, 0.2, 0.4, 0.8, and 1 mA cm^{-2}. b) Cyclic voltammograms for CNTs-SiW_{11} with a scan rate of 0.1 mVs^{-1} in the potential range 0–3 V.

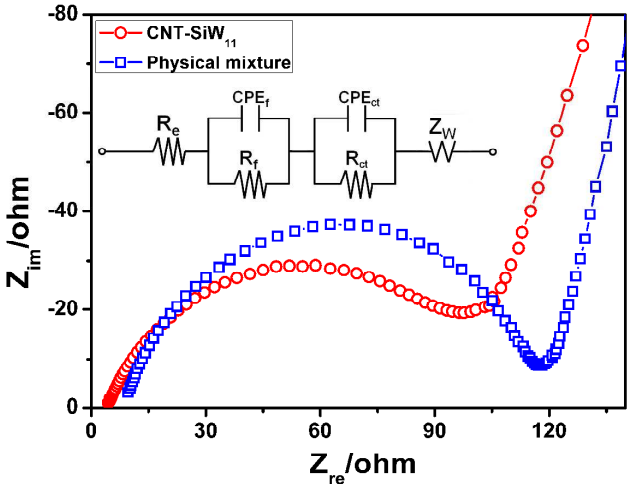

Fig. 8 Nyquist plots of the CNT-SiW_{11} nanocomposite, the physical mixture electrode, and the randles equivalent circuit for the CNT-SiW_{11} nanocomposite and the physical mixture electrode/electrolyte interface.

To take insight into the prominent electrochemical behavior of the CNTs-SiW_{11} electrode with respect to the physical mixture electrode, the AC impedance measurements is carried out for the each fresh coin cell. As shown in Figure 8, Nyquist plots of each cell in the frequency range of 10^{-2} to 10^5 Hz at the very potentials of 2.4V in the open voltage circuit are shown. To study the internal resistance of the test system, the equivalent circuit model is established as the inserted graph in Figure 8. In the model, R_e is the electrolyte resistance, R_f is the resistance of the surface film formed on the electrode R_{ct} is the charge-transfer resistance inside the battery, CPE_f and CPE_{ct} represent the constant phase element, and Z_W is the Warburg impedance related to the diffusion of lithium ions into the bulk electrodes. It can be seen that both plots are consisted of a semi-circle in the high-middle frequency region related to the impedance behaviour of surface film and charge-transfer processes, and a nearly vertical line following the first semi-circle in the low frequency region related to the ion diffusion processes. Fitting by the equivalent circuit model, the values of surface film resistance (R_f) and charge-transfer resistance (R_{ct}) are 94.77 and 209.6 Ω for the CNTs-SiW_{11} electrode, respectively. These values are lower than those of the physical mixture electrode (111.3 and 1282 Ω), which indicates that connecting POMs to CNTs *via* covalent bond can not only provides more pathways for the lithium diffusion, but also results in better electrochemical performances of CNTs toward lithium during the lithium intercalation/extraction reaction.

Conclusions

In summary, the connection of SiW_{11}-NH_2 to CNTs *via* covalent bonds for the first time results in the formation of new CNTs-SiW_{11} nanocomposite material. Investigation of the CNTs-SiW_{11} nanocomposite as anode material at a current density of 0.5 mA cm^{-2} exhibits the discharge capacity of 650 mAh g^{-1}, which remains stable for up to at least 100 cycles. The electrochemical performance of the CNTs-SiW_{11} nanocomposite can be attributed to the formation of sidewall defects of CNTs by introducing SiW_{11} covalently, which shorten the diffusion length of lithium ions and enable effective electron transfer. This study provides the first example of POMs modified CNTs by the formation of amide bond, and opens a new pathway for the preparation of CNTs-based advanced anode materials.

Acknowledgements

This research was supported by the National Science Foundation of China (21222104), the Fundamental Research Funds for the Central Universities (RC1302) and the Program for Changjiang Scholars and Innovative Research Team in University.

Notes and references

State Key Laboratory of Chemical Resource Engineering Beijing University of Chemical Technology, Beijing 100029 (China)Address, Tel/Fax: (+)861064431832

E-mail: songyufei@hotmail.com or songyf@mail.buct.edu.cn
Homepage: http://sci.buct.edu.cn/szll/jsml/wlhxx/9778.htm
[†]These authors contributed equally to this work.

††Electronic Supplementary Information (ESI) available: [details of any supplementary information available should be included here]. See DOI: 10.1039/b000000x/

1. a) J. C. Charlier and J. P. Issi, *Appl. Phys. A,* 1998, **67**, 79; b) A. Bachtold, P. Hadley, T. Nakanishi and C. Dekker, *Science,* 2001, **294**, 1317.
2. a) R. H. Baughman, A. A. Zakhidov and W. A. de Heer, *Science,* 2002, **297**, 787; b) M. F. L. De Volder, S. H. Tawfick, R. H. Baughman and A. J. Hart, *Science,* 2013, **339**, 535; c) Z. Liu, M. Winters, M. Holodniy and H. Dai, *Angew. Chem.,* 2007, **119**, 2069; *Angew. Chem. Int. Ed.,* 2007, **46**, 2023; d) Z. Wu, Z. Chen, X. Du, J. M. Logan, J. Sippel, M. Nikolou, K. Kamaras, J. R. Reynolds, D. B. Tanner, A. F. Hebard and A. G. Rinzler, *Science,* 2004, **305,** 1273.
3. a) A. Hirsch, *Angew. Chem.,* 2002, **114**, 1933; *Angew. Chem. Int. Ed.,* 2002, **41**, 1853; b) K. Balasubramanian and M. Burghard, *Small,* 2005, **1**, 180; c) D. Tasis, N. Tagmatarchis, A. Bianco and M. Prato, *Chem. Rev.,* 2006, **106**, 1105.
4. a) J. Chen, M. A. Hamon, H. Hu, Y. Chen, A. M. Rao, P. C. Eklund and R. C. Haddon, *Science,* 1998, **282**, 95; b) D. Tasis, N. Tagmatarchis, V. Georgakilas and M. Prato, *Chem.– A Eur. J.,* 2003, **9**, 4000.
5. a) F. M. Toma, A. Sartorel, M. Iurlo, M. Carraro, P. Parisse, C. Maccato, S. Rapino, B. R. Gonzalez, H. Amenitsch and T. Da Ros, *Nat. Chem.,* 2010, **2**, 826; b) R. Liu, S. Li, X. Yu, G. Zhang, Y. Ma and J. Yao, *J. Mater. Chem.,* 2011, **21**, 14917; c) F. Li, B. Zhang, X. Li, Y. Jiang, L. Chen, Y. Li and L. Sun, *Angew. Chem.,* 2011, **123**, 12484; *Angew. Chem. Int. Ed.,* 2011, **50**, 12276; d) D. M. Guldi, M. Marcaccio, D. Paolucci, F. Paolucci, N. Tagmatarchis, D. Tasis, E. Vázquez and M. Prato, *Angew. Chem.,* 2003, **115**, 4338; *Angew. Chem. Int. Ed.,* 2003, **42**, 4206; e). Y. Zhang, Y. Shen, J. Yuan, D. Han, Z. Wang, Q. Zhang and L. Niu, *Angew. Chem.,* 2006, **118**, 5999; *Angew. Chem. Int. Ed.,* 2006, **45**, 5867;
6. a) M. A. Hamon, J. Chen, H. Hu, Y. Chen, M. E. Itkis, A. M. Rao, P. C. Eklund and R. C. Haddon, *Adv. Mater.,* 1999, **11**, 834; b). K. Fu, W. Huang, Y. Lin, L. A. Riddle, D. L. Carroll and Y.–P. Sun, *Nano. Lett.,* 2001, **1**, 439.
7. a) D. Ma, L. Liang, W. Chen, H. Liu and Y.-F. Song, *Adv. Funct. Mater.,* 2013, **48,** 6100; b) M. Holzinger, O. Vostrowsky, A. Hirsch, F. Hennrich, M. Kappes, R. Weiss and F. Jellen, *Angew. Chem.,* **2001**, *113*, 4132-4136; *Angew. Chem. Int. Ed.,* 2001, **40**, 4002; c) J. L. Bahr, J. Yang, D. V. Kosynkin, M. J. Bronikowski, R. E. Smalley and J. M. Tour, *J. Am. Chem. Soc.,* 2001, **123**, 6536.
8. a) B. Z. Tang and H. Xu, *Macromolecules,* 1999, **32**, 2569; b) D. A. Britz and A. N. Khlobystov, *Chem. Soc. Rev.,* 2006, **35**, 637.
9. a) P. Yin, T. Li, R. S. Forgan, C. Lydon, X. Zuo, Z. N. Zheng, B. Lee, D. Long, L. Cronin and T. Liu, *J. Am. Chem. Soc.,* 2013, **135**, 13425; b) W. Chen, D. Ma, J. Yan, T. Boyd, L. Cronin, D.–L. Long and Y.–F. Song, *ChemPlusChem,* 2013, **78**, 1226; c) C. Yvon, A. Macdonell, S. Buchwald, A. J. Surman, N. Follet, J. Alex, D.–L. Long and L. Cronin, *Chem. Sci.,* 2013, **4**, 3810.
10. a) C. L. Hill, *Chem. Rev.*, 1998, **98**, 1; b) D. L. Long, E. Burkholder and L. Cronin, *Chem. Soc. Rev.,* 2007, **36**, 105; c) Y. F. Song, D. L. Long, C. Ritchie and L. Cronin, *Chem. Rev.,* 2011, **11**, 158; d) A. Dolbecq, E. Dumas, C. R. Mayer and P. Mialane, *Chem. Rev.,* 2010, **110**, 6009; e) L. Cronin and A. Müller, *Chem. Soc. Rev.,* 2012, **41**, 7333; f) C. Pan, D. Li and T. Liu, *Chem. Soc. Rev.,* 2012, **41**, 7368; g) Y. F. Song and R. Tsunashima, *Chem. Soc. Rev.,* 2012, **41**, 7384; h) A. Müller and P. Gouzerh, *Chem. Soc. Rev.,* 2012, **41**, 7431; i) A. Proust, B. Matt, R. Villanneau, G. Guillemot, P. Gouzerh and G. Izzet, *Chem. Soc. Rev.,* 2012, **41**, 7605.
11. a) D. Li, J. Song, P. Yin, S. Simotwo, A. Bassler, Y. Aung, J. E. Roberts, K. I. Hardcastle, C. L. Hill and T. Liu, *J. Am. Chem. Soc.,* 2011, **133**, 14010; b) T. Liu, E. Diemann, H. Li, A. W. M. Dress and A. Müller, *Nature,* 2003, **426**, 59; c) B. Keita and L. Nadjo, *Encyclopedia of Electrochemistry*, Wiley–VCH, Weinheim, 2006; d) J. Zhang, Y. F. Song, L. Cronin and T. Liu, *J. Am. Chem. Soc.,* 2008, **130**, 14408 .
12. X. M. Liu, Z. Huang, S. Oh, B. Zhang, P. C. MA, M. M. F. Yuen and J. K. Kim, *Compos. Sci. Technol*, 2012, **72**, 121.
13. F. M. Toma, A. Sartorel, M. Iurlo, M. Carraro, P. Parisse, C. Maccato, S. Rapino, B. R. Gonzolez, H. Amenitsch, T. D. Ros, L. Casalis, A. Goldoni, M. Marcaccio, G. Scorrano, G. Scoles, F. Paolucci, M. Prato and M. Bonchio, *Nat. Chem.,* 2010, **2**, 826.
14. a) A. Giusti, G. Charron, S. Mazerat, J. D. Compain, P. Mialane, A. Dolbecq, E. Rivière, W. Wernsdorfer, R. N. Biboum, B. Keita, L. Nadjo, A. Filoramo, J. P. Bourgoin and T. Mallah, *Angew. Chem.,* 2009, **121**, 5049; *Angew. Chem. Int. Ed.,* 2009, **48**, 4949 ; b) G. Charron, A. Giusti, S. Mazerat, P. Mialane, A. Gloter, F. Miserque, B. Keita, L. Nadjo, A. Filoramo, E. Rivière, W. Wernsdorfer, V. Huc, J. P. Bourgoin and T. Mallah, *Nanoscale,* 2010, **2**, 139.
15. N. Kawasaki, H. Wang, R. Nakanishi, S. Hamanaka, R. Kitaura, H. Shinohara, T. Yokoyama, H. Yoshikawa and K. Awaga, *Angew. Chem.,* 2011, **123**, 3533; *Angew. Chem. Int. Ed.*, 2011, **50**, 3471.
16. H. Wang, S. Hamanaka, Y. Nishimoto, S. Irle, T. Yokoyama, H. Yoshikawa and K. Awaga, *J. Am. Chem. Soc.,* 2012, **134**, 4918.
17. S. Yang, J. Huo, H. Song and X. Chen, *Electrochimica Acta,* 2008, **53**, 2238.
18. I. Bar–Nahum, H. Cohen, R. Neumann, *Inorg. Chem.,* 2003, **42**, 3677.
19. C. Gao, C. Vo, Y. Z. Jin, W. Li and S. P. Armes, *Macromolecules,* 2005, **38**, 8634.
20. a) Y. Yan, S. Yang, J. Cui, L. Jakisch, P. Pötschke and B. Voit, *Polym. Int.* 2011, **60**, 1425; b) W. Z. Yuan, Y. Mao, H. Zhao, J. Z. Sun, H. P. Xu, J. K. Jin, Q. Zheng and B. Z. Tang, *Macromolecules,* 2008, **41**, 701.
21. a) K. Flavin, K. Lawrence, J. Bartelmess, M. Tasior, C. Navio, C. Bittencourt, D. F. O Shea, D. M. Guldi and S. Giordani, *Acs Nano*, 2011, **5**, 1198; b) M. Sathiya, A. S. Prakash, K. Ramesha, J_M. Tarascon and A. K. Shukla, *J. Am. Chem. Soc*., 2011, **133**, 16291.